Communications in Physics, Vol. 25, No. 4 (2015), pp. 349-357
DOI:10.15625/0868-3166/25/4/5062

INFLUENCE OF POLYVINYL PYRROLIDONE ON ABSORPTION AND RADIATION TRANSITIONS OF Mn^{2+} IONS IN Mn-DOPED ZnS NANOPARTICLES

DANG VAN THAI, PHAM VAN THANG, PHAM VAN BEN, BUI HONG VAN
Hanoi University of Science, Vietnam National University, Hanoi
TRAN MINH THI
Hanoi National University of Education
HOANG NAM NHAT
Faculty of Engineering Physics and Nano Technology, University of Engineering and Technology, Vietnam National University, Hanoi

E-mail: nhathn@vnu.edu.vn

Received 29 November 2015
Accepted for publication 24 December 2015

Abstract. *ZnS:Mn nanoparticles were synthesized by co-precipitation method from the precursors solutions of 0.1M $Zn(CH_3COO)_2$, Na_2S and $Mn(CH_3COO)_2$ then were capped with polyvinyl pyrrolidone. The XRD patterns showed that the ZnS:Mn nanoparticles possessed the $T_d^2 - F4\bar{3}m$ cubic structure with the average crystallite size of several nanometers. At 300 K, the obtained photoluminescence spectra showed only a wide yellow-orange band centered at 603 nm, which should be attributed to the radiation transition of [$^4T_1(^4G) \rightarrow {}^6A_1(^6S)$] of $Mn^{2+}(3d^5)$ cations in the ZnS matrix. The excitation spectra recorded at 300 K on the other hand featured a strong photoluminescence band around 344 nm, which were assigned to the near band-edge absorption transition of ZnS host lattice, in addition with three weaker bands relating to the absorption transitions of [$^6A_1(^6S) \rightarrow {}^4T_2(^4D)$]: 430 nm, [$^6A_1(^6S) \rightarrow {}^4A_1(^4G) - {}^4E(^4G)$]: 468 nm, and [$^6A_1(^6S) \rightarrow {}^4T_2(^4G)$]: 492 nm of $Mn^{2+}(3d^5)$ cations. It was shown that the capping affected only the intensities of emissions bands.*

Keywords: nanoparticles, absorption, photoluminescence, photoluminescence excitation.

I. INTRODUCTION

Polyvinyl pyrrolidone (PVP) is a conductive polymer with a strong polarized carbonyl (–C=O) group, whose oxygen atom is capable to create bonds with both $Zn^{2+}(3d^{10})$ and $Mn^{2+}(3d^5)$ cations locating on the surface of ZnS:Mn nanoparticles [1, 2]. In the carbonyl group, the highest occupied molecular obitals (HOMO) are σ, n, π and lowest unoccupied molecular obitals (LUMO) are σ^*, n^*, π^*. Under ultraviolet radiation, the PVP chain's electrons can be excited to transit between HOMO and LUMO levels, then collide with host lattice and emit radiation [2]. Therefore, PVP is widely used as a surfactant in order to prevent agglomeration and stabilize particle size, while simultaneously increase the emission intensity of the host matrices [3, 4]. In this paper,

we present the study of influence of PVP binding on the excitation characteristics of ZnS:Mn nanoparticles prepared by mean of the co-precipitation technique.

II. EXPERIMENTALS

In order to synthesize ZnS:Mn/PVP nanoparticles, first we prepared the ZnS:Mn nanoparticles with Mn concentration $C_{Mn} = 8$ mol% by co-precipitation method as follows. By dissolving each of $Zn(CH_3COO)_2.2H_2O$, $Mn(CH_3COO)_2.4H_2O$ and Na_2S precursors with appropriate masses in twice-distilled water we achieved 0.1M solutions of $Zn(CH_3COO)_2$(A), $Mn(CH_3COO)_2$ (B) and Na_2S (C) which were stirred for 30 minutes. By mixing A with B (with defined volume ratios) and stirring for 30 minutes we obtained a solution with Mn concentration of 8 mol% (denoted as D). The C solution was then gradually dropped into D and stirred for the next 30 minutes to obtain the (ZnSMnS)$\downarrow$ precipitation by the reaction:

$$Zn(CH_3COO)_2 + Mn(CH_3COO)_2 + 2Na_2S \rightarrow (ZnSMnS)\downarrow + 4CH_3COONa$$

The precipitation was separated from the solute by using a centrifuge at 2500 prm and was filtered repeatedly with distilled water. After that the resultant was dried at 80˚C for 10 hours and ground. Finally the ZnS:Mn nanoparticles were obtained in the powder form. These nanoparticles were capped with PVP as follows. By disolving 0.5 g of ZnS:Mn powder in 10 ml of CH_3OH:H_2O with volume ratio 1:1 and with stirring for 1h we obtained E solution. By adding 0.1 g of PVP in to 10 ml of C_2H_5OH and with stirring for 1h we obtained F solution. E and F solutions were then mixed together and stirred for 2h to disperser the ZnS:Mn nanoparticles in PVP. By drying this solution at 80˚C for the next 10 h we obtained the final PVP-capped ZnS:Mn nanoparticles (denoted as ZnS:Mn/PVP) with PVP mass of 0.1 g. By the same route, the ZnS:Mn/PVP nanoparticles with different PVP mass were prepared, particularly with the same mass ZnS:Mn of 0.5g and mass of PVP changed from 0.1 to 0.9 g.

The crystalline structure and average crystalline size of ZnS:Mn/PVP nanoparticles were determined by X-ray diffraction pattern (XRD) recorded on XD8 Advance Bukerding using CuKα radiation ($\lambda = 1.5406$ Å, $2\theta = 10 - 70^{\circ}$) at room temperature. The morphology and average particle size were investigated by TEM using JEM-1010 facility. The thermal gravimetric analysis (TGA) and differential gravimetric analysis thermographs (DTG) were performed on Setaram instrumentation. Fourier transfer infrared absorption spectra (FT-IR) at 300 K were recorded on Nicolet 6700 FT-IR spectroscopy. UV-Vis spectra, photoluminescence (PL) and photoluminescence excitation (PLE) spectra of nanoparticles at 300 K were excited by radiations of deuterium, halogen and XFOR 450 xenon lamps, He-Cd laser and recorded on UV-Vis 2550, FL 3-22, Spectropro 2300i spectrometers, respectively.

III. RESULTS AND DISCUSSION

III.1. Crystalline structure and morphology of nanoparticles

Fig. 1 presents XRD patterns of ZnS:Mn/PVP ($C_{Mn} = 8$ mol%) nanoparticles with different PVP mass. These spectra include three diffraction peaks of (111), (220) and (311), in which (111) has greatest intensity. The XRD pattern shows that ZnS:Mn/ PVP nanoparticles were single-phased polycrystallites with $T_d^2 - F\bar{4}3m$cubic symmetry. The lattice constants and average

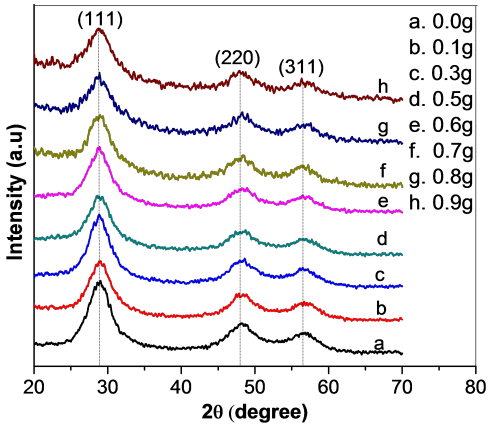

Fig. 1. XRD patterns of ZnS:Mn/PVP nanoparticles with different mass of PVP

crystallite size were determined from XRD patterns using the Debye-Sherrer formula [5]:

$$D = \frac{0.9\lambda}{\beta \cos\theta}, \tag{1}$$

where, λ (nm) is the wavelength of CuKα radiation; β (rad) the full width at haft maximum and θ (rad) the diffraction angle. The calculated results show that the lattice constants and average crystallite sizes of capped nanoparticles (with different PVP mass) were almost unchanged, $a = b = 5.370$ Å. This value is comparable to ZnS lattice constant given in (JCPDS Card. No. 05-0566, $a = b = 5.406$ Å). The average crystalline size was $\sim 3.5 - 3.6$ nm.

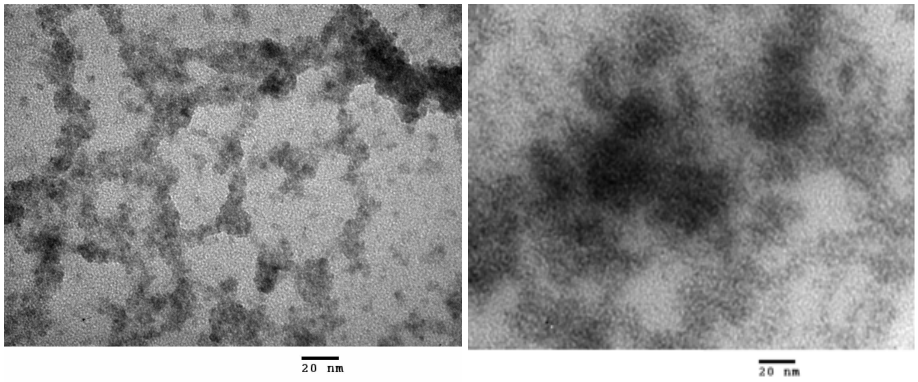

(a) (b)

Fig. 2. TEM images of ZnS:Mn (a) and ZnS:Mn/PVP nanoparticlers (m_{pvp} = 0.7 g) (b)

Fig. 2 presents the TEM images of ZnS:Mn and ZnS:Mn/PVP nanoparticles with PVP mass of 0.7 g. As showed, the ZnS:Mn nanoparticles agglomerated together to form the clusters with average size of 3.5 – 4 nm (Fig. 2(a)). This was mainly caused by the orientation of attachment of nanoparticles due to the static electrical force, van der Waals force and tension force [6]. When the nanoparticles were dispersed into PVP solution, the bonding coordination between –C=O group and Zn^{2+}, Mn^{2+} cations prevented the nanoparticles to agglomerate and helped to distribute them more uniformly with final average particle size of about 3–3.6 nm (Fig. 2(b)). These values were consistent with the ones calculated from the XRD patterns and Debye-Sherrer formula.

III.2. Analyses of TGA, DTG and FT-IR spectra

The PVP capping can be proved by investigation of TGA, DTG and FT-IR spectra. Fig. 3 shows TGA, DTG curves of PVP and ZnS:Mn/PVP ($m_{PVP} = 0.7g$) nanoparticles, the samples were annealed from 30 to 650-800 ˚C in argon atmosphere with heating rate of 10˚C/min. The curves showed three weight loss regions. For the PVP, the evaporation of water appeared in the temperature range from 30 to 120˚C with endothermic peak seen in the DTG curve at around 95˚C which was accompanied by a weight lose about of 14.4% (Fig. 3(a), 3(b)) [7]. In the temperature range from 120 to 500˚C, the fast decomposition of polymer chains of PVP could be seen clearly with a sharp endothermic peak at 440˚C in the DTG curve, the weight loss was 73.4 % (Fig. 3(a), 3(b)) [8]. Finally, other components were also decomposed in the temperature range from 500 to 650˚C with a weak endothermic peak seen around 550˚C in the DTG curve (Fig. 3(b)) [8].

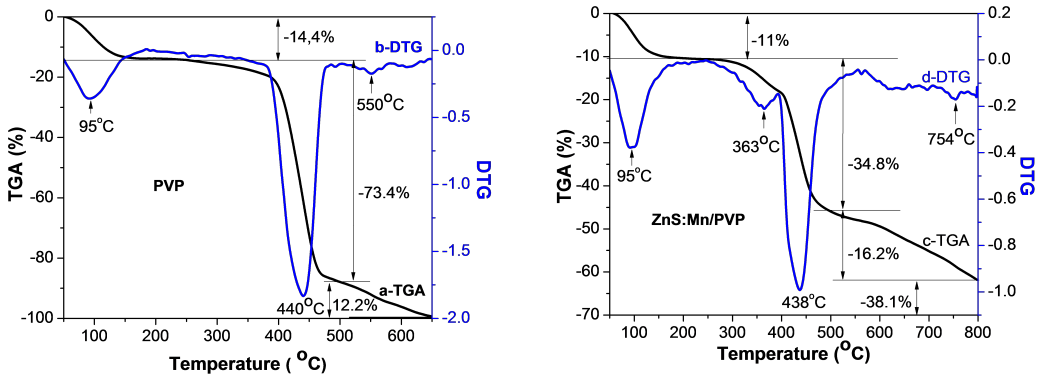

(a) **(b)**

Fig. 3. TGA and DTG spectra of PVP (a) and ZnS:Mn/PVP (b) nanoparticles (m_{PVP} = 0.7g)

For the ZnS:Mn/PVP nanoparticles, there occurred the weight losses in the temperature range from 30 to 500˚C due to water evaporation (11%) and PVP polymer chains decomposition (34.8%, see Fig. 3(c)). These can be seen from endothermic peaks at 95 and 438˚C in the DTG curve (Fig. 3(d)). The observed evidences showed that the ZnS:Mn nanoparticles were capped with PVP. Moreover, in the DTG curve there occurred weak endothermic peaks at 363˚C and 754˚C which should be assigned to the crystallite deformation and ZnS oxidation [9].

FT-IR spectrum of PVP (Fig. 4(a)) showed the bands which can be attributed to the stretching vibration of OH groups at 3445 cm^{-1}, C-H at 2960- 2871 cm^{-1}; C=O at 1656 cm^{-1}, C-N

at 1291, 1172 .... The CH bending vibration modes of CH_2 group can be recognized at 1465 and 1374 cm^{-1} [10–12]. Moreover, the vibrations characteristic to N-OH bonds occurred at 1230 cm^{-1}; to C-C bonds at 847 cm^{-1} and the stretching vibration of oxygen at 1000 cm^{-1} with smaller absorbance. For the PVP-capped ZnS:Mn nanopartilces with PVP mass of 0.7 g, the FI-IR spectrum showed the bands characteristic to PVP. In addition, it also showed lines typical for Zn-S at 1110, 471 cm^{-1} with weak absorbance [3]. However, the positions of almost all lines characteristic to PVP (in ZnS:Mn/PVP nanoparticles) were shifted towards the shorter wavenumber (the red shift) about 3-4 cm^{-1} (Fig. 4(b)). Notably, the red shifts were seen for C=O at 1647 cm^{-1}. This observation demonstrated that O atoms were coordinated with Zn^{2+}, Mn^{2+} cations on the surface of ZnS:Mn nanoparticles. Due to binding of PVP, and the lines attributed to the vibration of –C=O, OH groups were shifted towards the shorter wavenumber.

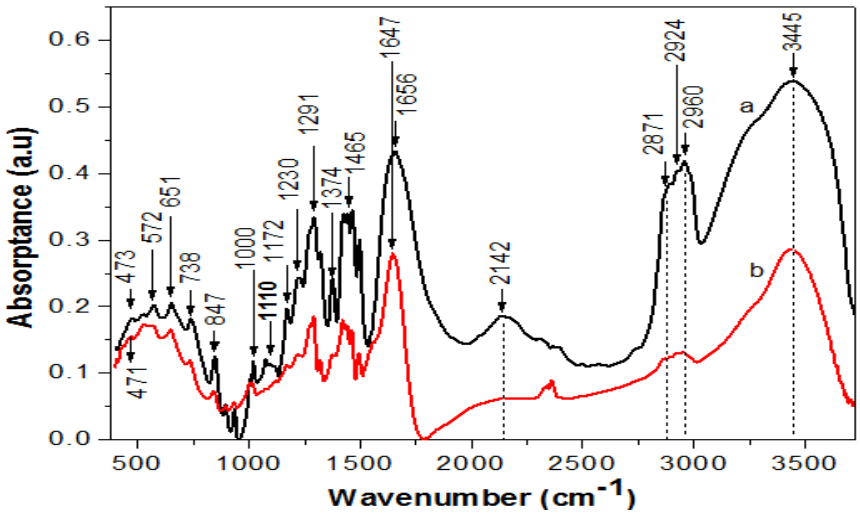

Fig. 4. FT-IR spectra of PVP (a), and ZnS:Mn/PVP nanoparticles ($m_{PVP} = 0.7$ g) (b)

III.3. The influence of PVP on absorption and radiation transitions of Mn^{2+} cations

The influence of PVP on absorption and radiation transitions of Mn^{2+} cations in capped nanoparticles can be observed in PL and PLE spectra. Fig. 5 shows the PL spectra of ZnS:Mn and capped nanoparticles with different PVP mass. The PL spectra of pure ZnS:Mn nanoparticles presents only a yellow-orange band at about 603 nm with strong intensity and wide width (Fig. 5(a)). This band should attribute to the radiation transition of $3d^5$ electrons from $^4T_1(^4G)$ excited state to $^6A_1(^6S)$ ground state of Mn^{2+} ions in ZnS host (refferred to as the Mn^{2+} radiation band) [13]. For PVP-capped nanoparticles the intensity of this yellow-orange band increased and reached the maximum at the PVP mass of 0.7 g (Fig. 5(b)-5(f)), then decreased until PVP mass equal 0.9 g (Fig. 5(g)- 5(h)). However, the positions of band remained unchanged. The intensity dependence of the yellow-orange band on capping PVP mass is presented in the inset of Fig. 5.

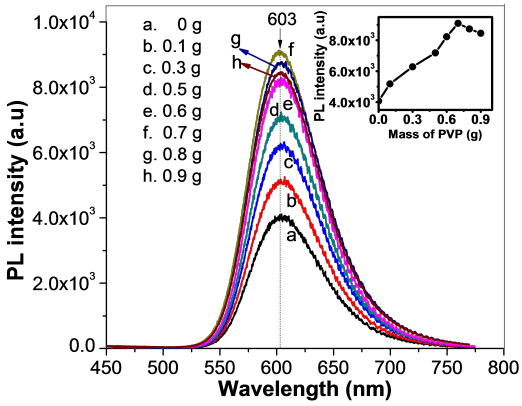

Fig. 5. PL spectra of ZnS:Mn/PVP nanoparticles with different PVP mass

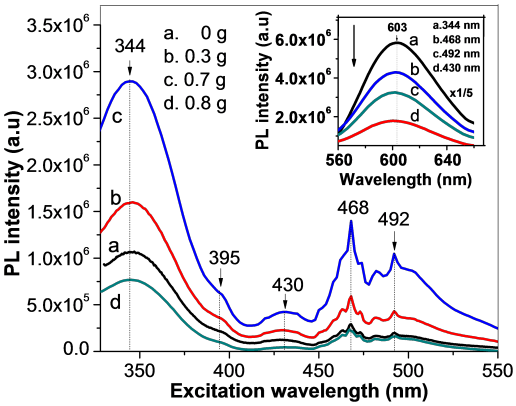

Fig. 6. PLE spectra when minitoring the yellow-orange band of ZnS:Mn/PVP nanoparticles with different PVP mass

Fig. 6 shows the PLE spectra while monitoring the yellow – orange band of ZnS:Mn/PVP nanoparticles with different PVP mass as excited by radiations of XFOR-450 lamp. For uncapped ZnS:Mn nanoparticles, the PLE spectra showed a wide band with strong intensity at 344 nm (Fig. 6(a)). This band should attribute to the near band-edge absorption transition of ZnS host, since its photon energy was near the value of ZnS band-gap [14]. Besides, there also appeared bands with smaller intensity at 395, 430, 468 and 492 nm (Fig. 6(a)). These bands could be assigned to the absorption transitions of $3d^5$ electrons from $^6A_1(^6S)$ ground state to $^4E(^4D)$, $^4T_2(^4D)$,$^4A_1(^4G)$-$^4E(^4G)$ and $^4T_2(^4G)$ excited states of Mn^{2+} cations in ZnS host lattice, respectively [15]. For PVP-capped ZnS:Mn nanoparticles with mass from 0.3 to 0.8 g, the intensity of these bands increased and achieved the maximum at mass equal 0.7 g (see Fig. 6(b),6(c)), afterwards it decreased until PVP-mass equal 0.8 g, with positions almost unchanged (Fig. 6(d)). The radiations of Xenon at 344, 430, 468, and 492 nm, corresponding to the near band edge absorption band and Mn^{2+} absorption bands, were used to excite ZnS:Mn/PVP nanoparticles with PVP mass of 0.7 g. The result showed that the position of yellow-orange band was also unchanged, but its intensity depended on excitation wavelengths. The intensity of this band was greatest when excited by 344 nm radiation, then decreased for 468, 492 nm excitation and achieved the lowest value when excited by 430 nm radiation (see the insert of Fig. 6). The unchanged position of the yellow- orange band can be considered also as the evidence for the occurrence of Mn^{2+} cations in the ZnS host lattice.

The PLE and PL spectra of ZnS:Mn/PVP nanoparticles excited by different excitation wavelengths showed that in these nanoparticles there exhibited two excitation mechanisms: the indirect excitation through ZnS host and the direct excitation of 3d-electrons of Mn^{2+} cations [15]. The excitation by 344 nm radiation with photon energy near the band gap energy of ZnS is mainly the indirect excitation. Meanwhile, excitation by 430, 468, 492 nm radiations with photon energy smaller than the band gap energy belongs to direct excitation mechanism. The probability of direct excitation was smaller than that of the indirect excitation. The above results showed that

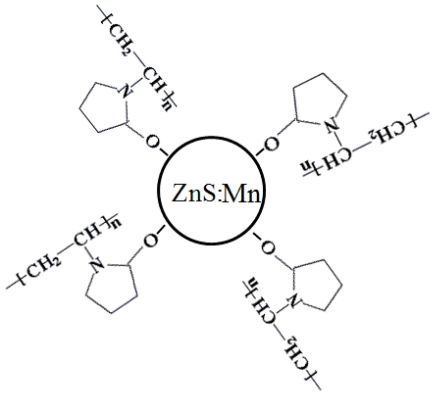

Fig. 7. PVP-capped ZnS:Mn nanoparticles model

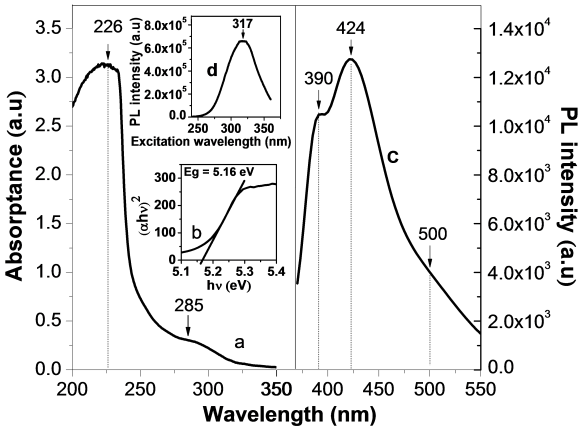

Fig. 8. Absorption spectrum (a), plot of $(\alpha h\nu)^2$ versus $(h\nu)$ (b), PL and PLE spectra (c,d) of PVP

for PVP-capped ZnS:Mn nanoparticles the intensity increase was due to PVP chains. PVP, with $(C_6H_9NO)_n$ molecular formula, is a conductive polymer possessing strong polarization carbonyl groups. When ZnS:Mn nanoparticles were disperted in PVP solution, the carbonyl groups were coordinated to Zn^{2+} and Mn^{2+} to form –C=O–Zn^{2+} and –C = O–Mn^{2+} bonds (Fig. 7), so preventing the agglomeration [1,2,6]. There also occurred a strong mixing between s-p states of ZnS host and 3d orbitals of Mn^{2+} cations [13], so the excitation energy transfer from ZnS host to Mn^{2+} sites became more effectively which in turn induced a higher intensity of yellow - orange band characteristic to Mn^{2+} cations [13]. In the cacbonyl group of PVP chains, the highest occupied molecular obitals (HOMO) are σ, n, π and the lowest unoccupied molecular obitals (LUMO) are σ^*, n^*, π^*. The absorption and radiation transitions between these obitals have the fingerprints in the UV-Vis and PL spectra. The UV-Vis spectra showed a band at 226 nm (5.48 eV) with large absorptance and a band at 285 nm (4.35 eV) with smaller absorptance (Fig. 8(a)). These bands can be assigned to the absorption transitions of electrons from $S_o(\pi)$, S_o(n) HOMO obitals to $S_1(\pi^*)$ LUMO orbital in –C = O group [1,2]. The band gap energy can be determined by using UV-Vis spectra and the Tauc relation [16]:

$$\alpha(h\nu) = A.(h\nu - E_g)^{\frac{1}{2}} \tag{2}$$

where α is absorptance, E_g (eV) the direct band gap energy, A a constant and $h\nu$ the photon energy. E_g can be evaluated via a plot of $(\alpha\ h\nu)^2$ versus $(h\nu)$, followed by an extrapolation of the linear portions of curves to the energy axis. For PVP, the band gap energy assigned to $[S_0(\pi) \rightarrow S_1(\pi^*)]$ transition has been determined of about 5.16 eV (Fig. 8(b)). This value was larger than the band gap energy of ZnS:Mn/PVP nanoparticles. The PL spectra of PVP solution ($C = 41.2\%$) at 300 K excited by 325 nm radiation of He-Cd laser present bands at 390, 424 and 500 nm, in which band at 424 nm has strongest intensity (Fig. 8(c)). In PLE spectra when monitoring 390 nm band of PVP mainly presented a band at 317 nm (3.91 eV) with strong intensity (Fig. 8(d)).

This band is characteristic to absorption transition of electrons from $S_o(n)$ HOMO orbital to $T_1(\pi^*)$ LUMO orbital in C=O group of PVP chains [2]. Under the effect of 325 nm (3.81 eV) radiation of He-Cd laser, the electrons of C=O group can absorb photons and then transit between $S_o(n)$ and $T_1(\pi^*)$ obitals and transfer their excitation energy to Mn^{2+} sites. This energy transfer also contributed to the intensity increase of bands which were attributed to the Mn^{2+} cations in PL and PLE spectra [2]. When capping PVP mass grew, the interaction of PVP chains and ZnS:Mn nanoparticles increased, but the interaction of PVP chains together reduced. These interactions could reduce the absorption and radiation transitions in Mn^{2+} sites, so the intensity of bands reduced [17]. The schema for absorption, radiation transitions of PVP, ZnS:Mn/PVP nanoparticles and excitation energy transfer from PVP to nanoparticles is present in Fig. 9.

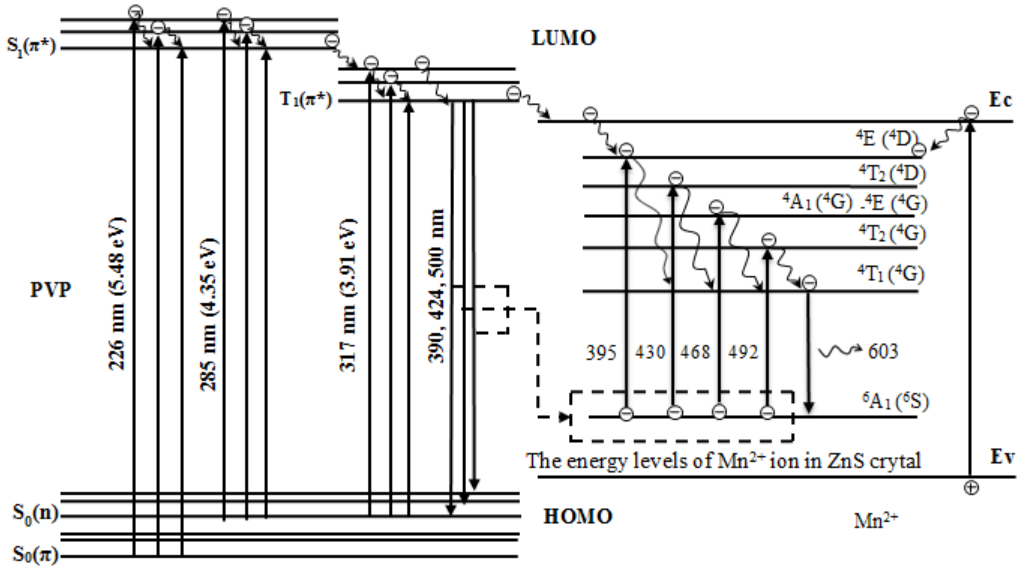

Fig. 9. Schema for absorption, radiation transitions of PVP, ZnS:Mn/PVP and excitation energy transfer from PVP into ZnS:Mn/PVP nanoparticles

IV. CONCLUSION

ZnS:Mn/PVP nanoparticles were prepared by dispersing ZnS:Mn into PVP solution. The coordination binding between –C=O carbonyl groups of PVP chains with Zn^{2+} and Mn^{2+} cations on the surface of ZnS:Mn nanoparticles formed the –C=O–Zn^{2+}; –C=O–Mn^{2+} bonds surrounding the nanoparticles themselves. Due to this, the excitation energy transfer from ZnS host and PVP chains to Mn^{2+} sites appeared more effective. This is the main cause for the increase of intensity of bands attributed to Mn^{2+} sites of ZnS:Mn/PVP nanoparticles in PLE and PL spectra.

AKNOLEGMENT

This research is funded by Vietnam National Foundation for Science and Technology Development (NAFOSTED) under grant number 103.02-2013.49

REFERENCES

[1] M. Klessinger and J. Michl, *Excited states and photochemistry of organic molecules*, VCH, 1995.
[2] K. Manzoor, S. Vadera, N. Kumar, and T. Kutty, *Solid State Communications* **129** (7) (2004) 469–473.
[3] G. Murugadoss, *Journal of Luminescence* **130** (11) (2010) 2207–2214.
[4] M. Chitkara, K. Singh, I. S. Sandhu, and H. S. Bhatti, *Nanoscale Research Letters* **6** (1) (2011) 438.
[5] A. Guinier, *X-ray diffraction*, Freeman, San Fran-cisco, 1963.
[6] J. Zhang, F. Huang, and Z. Lin, *Nanoscale* **2** (1) (2010) 18–34.
[7] N. M. Al-Hada, E. B. Saion, A. H. Shaari, M. A. Kamarudin, M. H. Flaifel, S. H. Ahmad, and S. A. Gene, *PloS one* **9** (8) (2014) e103134.
[8] D. C. Onwudiwe, T. P. Krüger, A. Jordaan, and C. A. Strydom, *Applied Surface Science* **321** (2014) 197–204.
[9] V. Ramasamy, K. Praba, and G. Murugadoss, *Superlattices and Microstructures* **51** (5) (2012) 699–714.
[10] H. Wang, X. Qiao, J. Chen, X. Wang, and S. Ding, *Materials Chemistry and Physics* **94** (2) (2005) 449–453.
[11] R. Mohan, S. Sankarrajan, and P. Santham, *International Journal of Recent Scientific Research* **4** (2013) 420–424.
[12] C. I. Covaliu, I. Jitaru, G. Paraschiv, E. Vasile, S.-Ş. Biriş, L. Diamandescu, V. Ionita, and H. Iovu, *Powder Technology* **237** (2013) 415–426.
[13] R. Bhargava, D. Gallagher, X. Hong, and A. Nurmikko, *Physical Review Letters* **72** (3) (1994) 416.
[14] A. Cadiş, E. Popovici, E. Bica, I. Perhaiţ, L. Barbu-Tudoran, and E. Indrea, *Chalcogenide Letters* **7** (11) (2010) 631–640.
[15] W. Chen, R. Sammynaiken, Y. Huang, J.-O. Malm, R. Wallenberg, J.-O. Bovin, V. Zwiller, and N. A. Kotov, *Journal of Applied Physics* **89** (2) (2001) 1120–1129.
[16] R. Seoudi, A. Shabaka, W. Eisa, B. Anies, and N. Farage, *Physica B: Condensed Matter* **405** (3) (2010) 919–924.
[17] G. Murugadoss, B. Rajamannan, and V. Ramasamy, *Digest journal of Nanomaterials and Biostructures* **5** (2) (2010) 339–345.